



Evaluation of titanium dioxide nanocrystal-induced genotoxicity by the cytokinesis-block micronucleus assay and the *Drosophila* wing spot test

Érica de Melo Reis^a, Alexandre Azenha Alves de Rezende^a, Pollyanna Francielli de Oliveira^b, Heloiza Diniz Nicolella^b, Denise Crispim Tavares^b, Anielle Christine Almeida Silva^c, Noelio Oliveira Dantas^c, Mário Antônio Spanó^{a,*}

^a Laboratório de Mutagênese, Instituto de Genética e Bioquímica, Universidade Federal de Uberlândia, Uberlândia, MG, 38400-902, Brazil

^b Universidade de Franca, Franca, SP, 14404-600, Brazil

^c Laboratório de Novos Materiais Isolantes e Semicondutores (LNMS), Instituto de Física, Universidade Federal de Uberlândia, Uberlândia, MG, 38400-902, Brazil

ARTICLE INFO

Article history:

Received 23 November 2015

Received in revised form

18 August 2016

Accepted 19 August 2016

Available online 22 August 2016

Keywords:

In vitro

In vivo

Mutagenicity

Nanotoxicology

Titania

Titanium (IV) oxide

ABSTRACT

Titanium dioxide nanocrystals (TiO₂ NCs) crystalline structures include anatase, rutile and brookite. This study evaluated the genotoxic effects of 3.4 and 6.2 nm anatase TiO₂ NCs and 78.0 nm predominantly rutile TiO₂ NCs through an *in vitro* micronucleus (MN) assay using V79 cells and an *in vivo* somatic mutation and recombination test in *Drosophila* wings. The MN assay was performed with nontoxic concentrations of TiO₂ NCs. Only anatase (3.4 nm) at the highest concentration (120 μM) induced genotoxicity in V79 cells. In the *in vivo* test, *Drosophila melanogaster* larvae obtained from standard (ST) or high bioactivation (HB) crosses were treated with TiO₂ NCs. In the ST cross, no mutagenic effects were observed. However, in the HB cross, TiO₂ NCs (3.4 nm) were mutagenic at 1.5625 and 3.125 mM, while 78.0 nm NCs increased mutant spots at all concentrations tested except 3.125 mM. Only the smallest anatase TiO₂ NCs induced mutagenic effects *in vitro* and *in vivo*. For rutile TiO₂ NCs, no clastogenic/augenetic effects were observed in the MN assay. However, they were mutagenic in *Drosophila*. Therefore, both anatase and rutile TiO₂ NCs induced mutagenicity. Further research is necessary to clarify the TiO₂ NCs genotoxic/mutagenic action mechanisms.

© 2016 Elsevier Ltd. All rights reserved.

1. Introduction

Titanium dioxide (TiO₂), titanium (IV) oxide, or titania is the naturally occurring oxide of titanium (Di Carlo et al., 2014; Grabowska et al., 2014). TiO₂ nanocrystals (NCs) are the most prevalent NCs in day-to-day use. Four naturally occurring TiO₂ NCs exist: rutile, anatase, brookite and titanium dioxide (B) (Banfield and Veblen, 1992). They are present in electronics, inks, food colorings, coatings for drugs and vitamins and several types of personal care products, such as toothpastes, sunscreens, soaps and shampoos (Chen et al., 2014; Weir et al., 2012; Yu and Li, 2011). One

of the major applications of TiO₂ NCs is their use as effective physical absorbers of UV rays in sun protection agents (Strobel et al., 2014). Nanoscale TiO₂ is more efficient in filtering UV light compared with the microscale counterparts (Smijs and Pavel, 2011). Furthermore, its use makes sunscreens more transparent, without opaqueness and with better tactile sensation (Newman et al., 2009).

The main feature of nanoscale products that makes them widely applicable is their reduced size. However, with decreased size there is an increase in their surface area to mass ratio, which makes them more reactive than the conventional formulation of the same product. Previous studies have shown that TiO₂ NCs can cause inflammation, pulmonary damage, fibrosis and lung tumors in rodents. Harmful interactions of NCs with biological systems and the environment raise concerns about their toxic/genotoxic potential (Chen et al., 2014; Cowie et al., 2015; Foth et al., 2012; Lindberg

* Corresponding author. Universidade Federal de Uberlândia, Instituto de Genética e Bioquímica, Laboratório de Mutagênese, Av. Pará 1720, Umuarama, Uberlândia, MG 38400-902, Brazil.

E-mail address: maspano@ufu.br (M.A. Spanó).

et al., 2012; Weir et al., 2012). Other parameters that can influence the toxic/genotoxic potential of TiO₂ NCs are the crystalline structure and chemical concentration (Fu et al., 2014; Jiang et al., 2008). Appropriate risk assessment in relation to health and safety of NCs used in medicine is essential, in order to ensure ethical, societal and regulatory acceptance, and public confidence (Juillerat et al., 2015).

TiO₂ was classified by the International Agency for Research on Cancer (IARC) as possibly carcinogenic to humans (IARC, 2010). Due to these data and the increasing risk of human exposure to NCs, investigations into the genotoxicity and mutagenicity aimed at understanding the safety of TiO₂ NCs are necessary to establish associations between their physicochemical properties and toxic effects (Carmona et al., 2015; Jiang et al., 2008; Landsiedel et al., 2009; Li et al., 2014; Strobel et al., 2014; Zhang et al., 2013). Based on the importance of TiO₂ NCs, we tested the hypothesis that size could be related to toxicity and mutagenicity.

TiO₂ NCs can be internalized into the cytoplasm and the cell nucleus, as demonstrated by Shukla et al. (2013) in human hepatocellular carcinoma cells (HepG2) using flow cytometry and transmission electron microscopy (TEM). That study also listed the possible mechanisms of toxicity induction, highlighting markers of oxidative stress and apoptosis.

Micronuclei (MN) are derived from chromosomal fragments and whole chromosomes that were retained in anaphase (Fenech, 2007). The MN can be evaluated by the cytokinesis-block micronucleus (CBMN) assay, which blocks the cell cycle using the cytokinesis block cytochalasin B, which produces binucleated cells, allowing a more accurate MN score and excluding the dividing cells from the non-dividing cells to enhance the reliability by reducing the incidence of false positive data (Deepa Parvathi and Rajagopal, 2014). The micronucleus test (MNT) has been used to evaluate clastogenic and aneugenic effects of different compounds, including nanoscale TiO₂ (Dobrzynska et al., 2014; Tavares et al., 2014).

In vivo studies offer many advantages, such as the study of the bioavailability of NCs to sensitive target cells and can increase the knowledge on the possible genotoxic potential risk associated with NCs exposure (Demir et al., 2011). Nevertheless, the commonly used *in vivo* mammalian tests appear to be ill adapted to tackle the large compound sets involved, due to throughput, cost, and ethical issues. Non-mammalian animals, such as *Drosophila melanogaster* are good candidates for the development of high-throughput genotoxicity tests due to their quick reproductive cycles, greater ethical acceptance, and smaller need for infrastructure (Lombardot et al., 2015). Besides, *Drosophila* is a well studied genetic model organism for understanding molecular mechanisms of human diseases. Nearly 75% of human disease-causing genes are believed to have a functional homolog in the fly (Pandey and Nichols, 2011). So, we used *Drosophila* Somatic Mutation And Recombination Test (SMART) (Graf and van Schaik, 1992; Graf et al., 1984) as a model for the study of the mutagenic/recombinogenic risks associated with TiO₂ exposure. The wing SMART assay, considered one of the gold standards for mutagenicity, can assess loss of heterozygosity (LOH) as a consequence of gene mutation, chromosome breaks/rearrangement or chromosome loss of suitable gene markers that have detectable wing phenotypes (Graf et al., 1984). Many hundreds of chemicals have already been tested using SMART, including NCs (Carmona et al., 2015; de Andrade et al., 2014; Demir et al., 2011, 2013; Reis et al., 2015; Vales et al., 2013).

The aim of the present study was to evaluate the genotoxic and mutagenic potentials of three types of TiO₂ NCs using the *in vitro* CBMN assay in Chinese hamster lung fibroblast cells (V79) and the *in vivo* wing SMART assay in *D. melanogaster*.

2. Materials and methods

2.1. Chemicals

The three types of TiO₂ nanocrystals (NCs) used in this study were designated as follows: anatase TiO₂ NCs of 3.4 nm (A3.4 TiO₂), anatase TiO₂ NCs of 6.2 nm (A6.2 TiO₂) and a mixture of rutile (64%)/brookite (35%)/anatase (1%) TiO₂ NCs of 78.0 nm (R78.0 TiO₂). All TiO₂ NCs were provided, synthesized and characterized at the Laboratory New Insulating Materials and Semiconductors (LNMIS), Physics Institute, Federal University of Uberlândia, Uberlândia, MG, Brazil. HAM-F10; DMEM; streptomycin (CAS 3810-74-0); penicillin (CAS 113-98-4); Hepes (CAS 7365-45-8); dimethyl sulfoxide (DMSO; CAS 67-68-5); methyl methanesulfonate (MMS; CAS 66-27-3); cytochalasinB (CAS 14,930-96-2), HNO₃, Ti(OCH(CH₃)₂)₄ and NaOH were purchased from Sigma-Aldrich. Ethyl carbamate (Urethane - URE; CAS: 51-79-6) was from Fluka AG, (Buchs, Switzerland) and fetal bovine serum from Nutricell (Campinas, SP, Brazil). As an alternative to *Drosophila* medium, instant mashed potato flakes (Yoki[®] Alimentos S. A., São Bernardo do Campo, SP, Brazil) were used. The solutions were always prepared immediately before use with ultrapure water obtained from a MilliQ system (Millipore, Vimodrome, Milan, Italy).

2.2. Synthesis and characterization of TiO₂ NCs

The TiO₂ NCs were synthesized in aqueous solution at room temperature as follows. A solution containing 300 mL of ultrapure water and 90 mL of nitric acid (HNO₃, 70%, Sigma Aldrich) under magnetic stirring for 20 min was added to 60 mL of titanium isopropoxide (Ti(OCH(CH₃)₂)₄, 97%). The pH of this solution was adjusted to 5.6 using 4 M sodium hydroxide (NaOH, 98%). The resulting solution was left to stand to precipitate TiO₂ NCs. The precipitate was monodispersed in ultrapure water under magnetic stirring and centrifuged at 6000 rpm for 10 min. Finally, the resulting precipitate purified from this solution was subjected to the following successive thermal treatments in ambient atmosphere: (i) 100 °C/24 h, (ii) 500 °C/1 h and (iii) 800 °C/1 h.

The High-resolution transmission electron microscopy (HRTEM) images were obtained by high-resolution transmission electron microscopy of accelerating voltage 200 kV, JEOL SIOD. The X-ray diffraction (XRD) was recorded with a DRX-6000 (Shimadzu) using monochromatic radiation Cu-K_{α1} ($\lambda = 1.54,056 \text{ \AA}$) to confirm the formation of TiO₂ NCs, as well as the crystal structure, size and average mass fraction of the rutile phase. The size of the NCs was estimated based on the Debye-Scherrer equation (Guinier, 1963). The XRD patterns of the samples treated at 100 °C/24 h and 500 °C/1 h used the (101) Bragg diffraction peak of the anatase phase located at approximately $2\theta = 25.4^\circ$, and samples treated at 800 °C/1 h used the peak (110) of the rutile phase located at approximately $2\theta = 27.8^\circ$. The percentage of anatase, brookite and rutile phases were calculated based on the literature (Koo et al., 2006; Yu et al., 2003). The micro-Raman spectra were obtained using as excitation source the 780 nm line of an Ocean Optics spectrometer. All characterizations were performed at room temperature. For the biological assays, the TiO₂ NCs were resuspended in distilled water to give the specific concentrations for each test and placed in ultrasound for 30 min for better dispersion of the particles.

2.3. *In vitro* assays

2.3.1. Cell line and culture conditions

Chinese hamster lung fibroblasts (V79 cells) were maintained as monolayers in plastic culture flasks (25 cm²) in HAM-F10 and DMEM (1:1) medium supplemented with 10% fetal bovine serum,

antibiotics (0.01 mg/mL streptomycin; 0.005 mg/mL penicillin), and 2.38 mg/mL Hepes at 36.5 °C in a BOD-type incubator. The average cell cycle time was 12 h under these conditions, and the experiments were carried out using V79 cells between the 6th and 12th culture passage after thawing. The protocols used in this study were performed in triplicate. The V79 cells were kindly supplied by Prof. Dr. I.M.S. Cólus – Universidade Estadual de Londrina, Londrina, PR, Brazil.

2.3.2. XTT colorimetric assay

The cytotoxic activity was evaluated using the *in vitro* colorimetric assay - XTT kit (Roche Diagnostics) according to the manufacturer's instructions. For the experiments, 1×10^4 cells were seeded into microplates containing 96 wells. Each well received a maximum of 100 µL of culture medium (DMEM + HAM F10 1:1) supplemented with 10% fetal bovine serum containing different concentrations of TiO₂ NCs (A3.4, A6.2 or R78.0). The concentrations tested ranged from 30.5 to 62,500.0 µM. Negative (no treatment) and positive (dimethylsulfoxide - DMSO 25%) controls were included in the microplates. After incubation with the compound for 24 h at 36.5 °C, the culture medium was removed and cells were washed with 100 µL of PBS to remove the compound and exposed to 100 µL of HAM-F10 medium red-free culture phenol. Then, 25 µL of XTT were added to each well. The microplates were incubated at 36.5 °C for 17 h. The sample absorbance was determined by means of a multi-plate reader (ELISA -Asys - UVM 340/MicroWIN 2000) at a wavelength of 450 nm and a reference length of 620 nm. The amount of soluble product (formazan) formed was proportional to the number of viable cells. The negative control group was designated as 100% and the results were expressed as a percentage of the negative control. The experiments were performed in triplicate.

2.3.3. Cytokinesis-block micronucleus (CBMN) assay

The V79 cells (500,000) were seeded into tissue-culture flasks and incubated for 25 h in 5 mL complete HAM-F10/DMEM medium and washed with PBS (pH 7.4). After the incubation, the cultures were rinsed with PBS and then submitted to one of the following treatments during 3 h: negative control (without treatment), A3.4 or A6.2 TiO₂ at concentrations of 30.0, 60.0 or 120.0 µM, R78.0 TiO₂ at 976.5, 1953.0 or 3906.0 µM, or positive control (MMS) at 400 µM. The concentrations of TiO₂ NCs were selected based on data obtained by the XTT colorimetric assay for cytotoxicity evaluation, whose results showed that the treatments with concentrations up to 244 µM for anatase TiO₂ NCs and up to 7812.0 µM for R78.0 TiO₂ showed statistically significant differences compared with the negative control, revealing cytotoxicity. All of the experiments were performed in triplicate. After the treatment period, the cells were washed with PBS and a culture medium supplemented with fetal bovine serum containing 3 µg/mL of cytochalasinB was added. The cells were incubated for 17 h. Then, the cells were rinsed with 5 mL PBS, trypsinized using 0.025% trypsin-EDTA and centrifuged for 5 min at 900 rpm. The pellet was hypotonized in sodium citrate 1% at 36.5 °C and then homogenized with a Pasteur pipette. This cell suspension was centrifuged again, the supernatant was discarded and the pellet was resuspended in methanol:acetic acid (3:1) and homogenized again with a Pasteur pipette. After fixation, the cells were stained in 5% Giemsa solution.

The analysis was established by Fenech (2000): 1000 cells were counted by culturing a total of 3000 binucleated cells per treatment. The nuclear division index (NDI) was determined for 500 cells analyzed per replicate, for a total of 1500 cells per treatment group using the same slides used on the micronucleus assay. Cells with well-preserved cytoplasm containing 1–4 nuclei were

scored, and the NDI was calculated using the following formula (Eastmond and Tucker, 1989):

$$NDI = \frac{[M1 + 2(M2) + 3(M3) + 4(M4)]}{N}$$

Where M1–M4 is the number of cells with 1, 2, 3 and 4 nuclei, respectively, and N is the total number of viable cells.

2.3.4. Statistical analysis - CBMN

The data were analyzed statistically by analysis of variance for completely randomized experiments, with calculation of F statistics and respective *p* values. In cases in which *p* < 0.05, treatment means were compared by the Tukey test and the minimum significant difference was calculated for 0.05.

2.4. In vivo assay

2.4.1. *D. melanogaster* strains and crosses

Three *D. melanogaster* strains with the genetic markers multiple wing hairs (*mwh*, 3–0.3) and flare-3 (*flr*³, 3–38.9) were kindly provided by the Physiology and Animal Husbandry Institute of Animal Sciences (University of Zurich, Schwerzenbach, Switzerland): (1) multiple wing hairs (*mwh/mwh*); (2) flare-3 (*flr*³/*ln(3LR)TM3, ri p^{sep} l(3)89Aa bx34^e and Bd^S*); and (3) ORR; flare-3 (*ORR/ORR; flr*³/*ln(3LR)TM3, ri p^{sep} l(3)89Aa bx34^e and Bd^S*). The ORR strain has chromosomes 1 and 2 from a DDT-resistant Oregon R(R) line, which are responsible for a high constitutive level of cytochrome P450 (Graf and van Schaik, 1992). These strains were maintained in glass vials filled with a maintenance medium (banana, sucrose, yeast and methylparaben) under light/dark cycles (12 h:12 h), at 25 ± 1 °C and approximately 60% humidity in a BOD-type chamber (Model: SL224, SOLAB – Equipamentos para Laboratórios Ltda., São Paulo, SP, Brazil).

Two crosses were carried out to produce the experimental larval progeny: (1) Standard (ST) cross, *mwh/mwh* males crossed with *flr*³/*ln(3LR)TM3, ri p^{sep} l(3)89Aa bx34^e and Bd^S* virgin females (Graf et al., 1984, 1989); (2) High bioactivation (HB) cross, *mwh/mwh* males crossed with *ORR/ORR; flr*³/*ln(3LR)TM3, ri p^{sep} l(3)89Aa bx34^e and Bd^S* virgin females (Graf and van Schaik, 1992). The two crosses produce two types of flies: marker *trans*-heterozygous (MH) flies (*mwh*^{+/+} *flr*³) and balancer-heterozygous (BH) flies (*mwh*^{+/+} *TM3, Bd^S*). The former has normal wings, while the latter can be distinguished phenotypically by its serrated wings.

2.4.2. Somatic mutation and recombination test – SMART

From the ST and HB crosses, eggs were collected for 8 h in culture bottles with 4% w/v agar-agar base topped with a thick layer of live baker's yeast supplemented with sucrose. Larvae of 72 ± 4 h were transferred to glass vials for a chronic feeding (approximately 48 h). Four sets of vials for each cross were prepared with 1.5 g of mashed potato flakes and 5 mL of a solution containing TiO₂ NCs (A3.4, A6.2 or R78.0) at concentrations of 1.5625, 3.125, 6.25, 12.5, 25.0, 50.0 and 100.0 mM. Negative (ultrapure water) and positive (URE 10 mM) controls were included in this experiment. The larvae were counted before distribution into two series of these vials to calculate the survival rates upon exposure. Larvae were allowed to feed on the above medium for the remainder of their development, to pupate and to hatch as adult flies. All experiments were conducted at 25 ± 1 °C and approximately 60% humidity.

The hatched flies were stored in 70% (v/v) ethanol. The wings of MH flies were removed and mounted in glass slides with Faure's solution (30 g gum Arabic, 20 mL glycerol, 50 g chloral hydrate, and 50 mL water) and analyzed for the size and frequency of spots under a compound microscope at 400× magnification.

Three types of spots can be observed on the wings of MH flies: (i) small single spots (*mwh* or *flr*³) consisting of one or two mutant hairs, resulting from deletions, point mutations, specific chromosome aberrations or from recombination between the two marker genes, (ii) large single spots (*mwh* or *flr*³) consisting of three or more hairs and (iii) twin spots (*mwh* and *flr*³) consisting of adjacent *mwh* and *flr*³ hairs, produced by somatic recombination between the proximal marker *flr*³ and the centromere of chromosome 3. Only *mwh* single spots can be recovered on the wings of BH flies. They are all due to mutational events, as recombinational events are suppressed due to the multiply inverted TM3 balancer chromosome (Graf et al., 1984; Guzmán-Rincón and Graf, 1995). For each analyzed wing, the three types of spots were recorded for further statistical analysis.

2.4.3. Statistical analysis

The experimental data were evaluated according to the multiple-decision procedure (Frei and Wurgler, 1988, 1995). The frequencies of each type of mutant clone per fly were compared with the concurrent negative control series using the conditional binomial test (Kastenbaum and Bowman, 1970), which is used to decide whether a result is positive, inconclusive or negative. Chi-square test was performed for statistical comparisons of survival rates for independent samples. Each statistical test was evaluated at the 5% significance level.

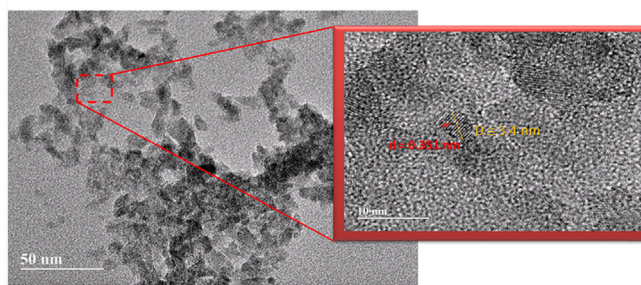
3. Results

3.1. Nanocrystal characterization

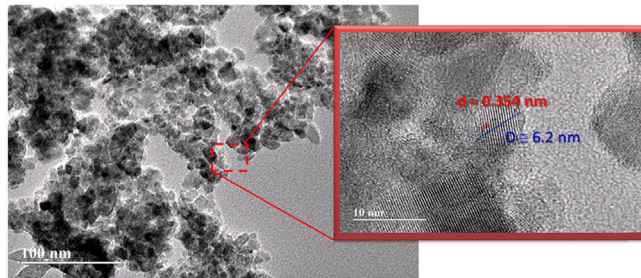
High-resolution transmission electron microscopy (HRTEM) was employed to investigate the size, phase and morphologies of TiO₂ NCs as illustrated in Fig. 1. In the left panels, show the nanoparticles with agglomerates. These agglomerates are due the high concentration used in measurements (1 mg/mL). The increased of thermal annealing favored the growth of nanoparticles. In the right panels observed the lattice fringes confirming the formation of nanocrystals. In Fig. 1A and B the NCs have a lattice spacing of 0.351 nm and 0.354 nm which corresponding to *d*₁₀₁ spacing of anatase TiO₂ crystal, respectively. In Fig. 1C observed that lattice spacing of NCs is 0.352 nm corresponding to *d*₁₁₀ spacing of rutile TiO₂ crystal. It is also observed the formation of other forms of nanocrystals providing indications of different phases. In addition, the average size of TiO₂ NCs are approximately 3.4, 6.2 and 78.0 nm to samples thermal annealing at 100 °C/24 h, 500 °C/1 h and 800 °C/1 h, respectively. These HRTEM images confirmed the formation of TiO₂ NCs and that the thermal annealing controls the phase of the nanocrystals.

In order to confirm the crystalline phase, the percentage of phases and that there is presence of contaminants were performed X-ray diffraction (XRD) and Raman spectroscopy, show in Fig. 2. Fig. 2A shows the X-ray diffraction (XRD) patterns of TiO₂ nanoparticles subjected to thermal annealing at 100 °C/24 h, 500 °C/1 h, and 800 °C/1 h. In the XRD pattern of sample with thermal annealing at 100 °C/24 h, observed the presence of Bragg diffraction peaks characteristic of TiO₂ anatase phase. The increase in thermal annealing from 100 °C to 500 °C did not alter the NCs crystalline phase. The increase in thermal annealing to 800 °C/1 h resulted in the transformation of anatase to rutile phase. This is because the increase in temperature enhancing the transformation of anatase, which is thermodynamically metastable, to the rutile phase that is more stable (Gaynor et al., 1997; Wu et al., 2002). Moreover, the diffractograms also demonstrated the presence of the brookite phase, which occurred due to the synthesis procedure used (Abbas et al., 2011; Pottier et al., 2001). Based on literature were calculate

A TiO₂ NCs 100 °C / 24 hr



B TiO₂ NCs 500 °C / 1 hr



C TiO₂ NCs 800 °C / 1 hr

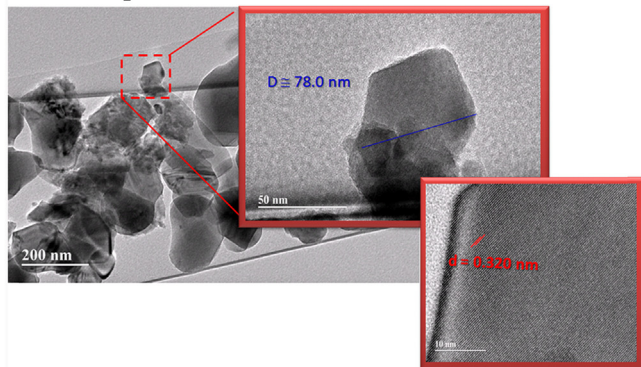


Fig. 1. HRTEM images of TiO₂ NCs thermal annealing at (A) 100 °C/24 h, (B) 500 °C/1 h and (C) 800 °C/1 h. In the left panels, show the nanoparticles with agglomerates and in the right panels observed the lattice fringes confirming the formation of TiO₂ nanocrystals.

the percentage of phases verifying a mixture 64% rutile, 35% brookite and 1% anatase phase (Koo et al., 2006; Yu et al., 2003). These observations in the XRD patterns are in excellent agreement with the HRTEM images. Fig. 2B shows the micro-Raman spectra of TiO₂ NCs. All spectra were normalized to the peak of greater intensity to facilitate the visualization of the active modes of the anatase, brookite and rutile phase present in the TiO₂ NCs. The TiO₂ NCs with thermal annealing at 100 °C/24 h exhibited the characteristic Raman bands of vibrations of anatase phase (Ohsaka, 1980; Zhang et al., 2000). The Raman band at approximately 144 cm⁻¹ was not visualized in the Raman system because detector used only detects in the range of 150–1000 cm⁻¹, observing the descent of the band. In the micro-Raman spectrum of the sample with thermal annealing at 500 °C/1 h, was also observed anatase phase modes. The increase in annealing temperature to 800 °C/1 h favored the formation of rutile and brookite, both observed in the Raman spectrum as well as in the XRD diffractogram (Fig. 1B). The absence of impurity peaks reinforces evidence that these TiO₂ NCs are of high purity.

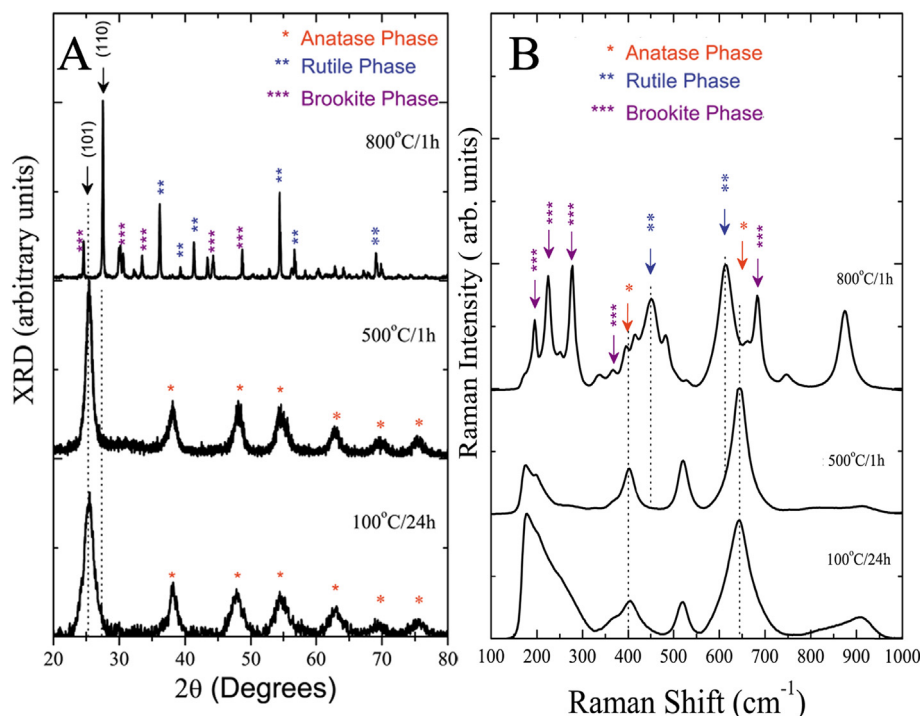


Fig. 2. (A) XRD patterns and (B) Raman spectra of TiO₂ NCs thermal annealing at 100 °C/24 h, 500 °C/1 h and 800 °C/1 h.

The three types of TiO₂ NCs used in this study were designated as anatase TiO₂ NCs of 3.4 nm (A3.4 TiO₂), anatase TiO₂ NCs of 6.2 nm (A6.2 TiO₂) and a mixture of rutile (64%)/brookite (35%)/anatase (1%) TiO₂ NCs of 78.0 nm (R78.0 TiO₂).

3.2. XTT colorimetric assay

The cytotoxicity of TiO₂ NCs (A3.4, A6.2 or R78.0) was assessed by XTT colorimetric assay in V79 cells at concentrations ranging from 30.5 to 62,500.0 μM. Fig. 3 shows the cell viability percentage of each treatment. The results demonstrated that treatments with A3.4 and A6.2 TiO₂ showed significant differences from negative control at concentrations higher than 122 μM (Fig. 3A–B, respectively). With R78.0 TiO₂, concentrations higher than 3.906 μM were considered statistically cytotoxic (Fig. 3C).

3.3. Micronucleus assay

The micronucleus (MN) frequency in V79 cells treated with 30, 60 or 120 μM A3.4 or A6.2 TiO₂, and 976.5, 1953.0 or 3906.0 μM R78.0 TiO₂ and the nuclear division index (NDI) are shown in Table 1. A3.4 TiO₂ significantly increased the frequency of MN at a higher concentration (120 μM), showing a genotoxic effect. No significant differences in MN induction were observed in the groups treated with 30 and 60 μM A3.4 TiO₂ when compared to negative control ($p > 0.05$). The results also demonstrated lack of genotoxic effects for A6.2 and R78.0 TiO₂, at all concentrations tested (Table 1).

Table 1 also displays the mean nuclear division index (NDI) and the respective standard deviation (SD) obtained for all treated groups. No significant differences were observed between the total induced MN in any treatment group compared to the negative control, demonstrating the absence of cytotoxicity of the different treatments under our experimental conditions.

3.4. Somatic mutation and recombination test – SMART

Third instar larvae of *D. melanogaster* obtained from ST and HB crosses were fed chronically with three different types of TiO₂ NCs: A3.4, A6.2 or R78.0, at concentrations ranging from 1.5625 to 100.0 mM. The survival rates are shown in Fig. 4. All concentrations tested were not toxic when compared to the negative control group. The assessment of size and frequency of spots was performed with the wings of flies treated with the four lowest concentrations tested (1.5625; 3.125; 6.25 or 12.5 mM).

The results of the wing spot test for the mutagenic evaluation of TiO₂ NCs (A3.4, A6.2 or R78.0) are summarized in Tables 2–4, for ST and HB crosses. As expected, the reference mutagen (URE) induced positive results for all spot categories in both crosses (ST and HB) compared to the negative control.

From the ST cross, TiO₂ NCs (A3.4, A6.2 or R78.0) at concentrations of 1.5625, 3.125, 6.25 or 12.5 mM did not significantly increase the frequency of mutant spots. Among HB individuals, A6.2 TiO₂ presented no genotoxic effect for any category of mutant spots recorded (Table 3). On the other hand, A3.4 and R78.0 TiO₂ induced mutagenic activity regardless of increasing dose.

4. Discussion

Studies on TiO₂ have revealed that the use of these NCs has both benefits and drawbacks. While TiO₂ NCs have been widely employed in industry, researchers worldwide have raised concerns about their potential genotoxic effects, which may be related to time and/or routes of exposure, crystalline structure, size, concentration.

Due to the extensive application of TiO₂ NCs in many commercial products, there are increased risks of exposure of human beings to these NCs. The routes of exposure can be via dermal penetration, inhalation, oral ingestion or intravenous injection (Shakeel et al., 2016). Studies on toxicological effects of TiO₂ NCs

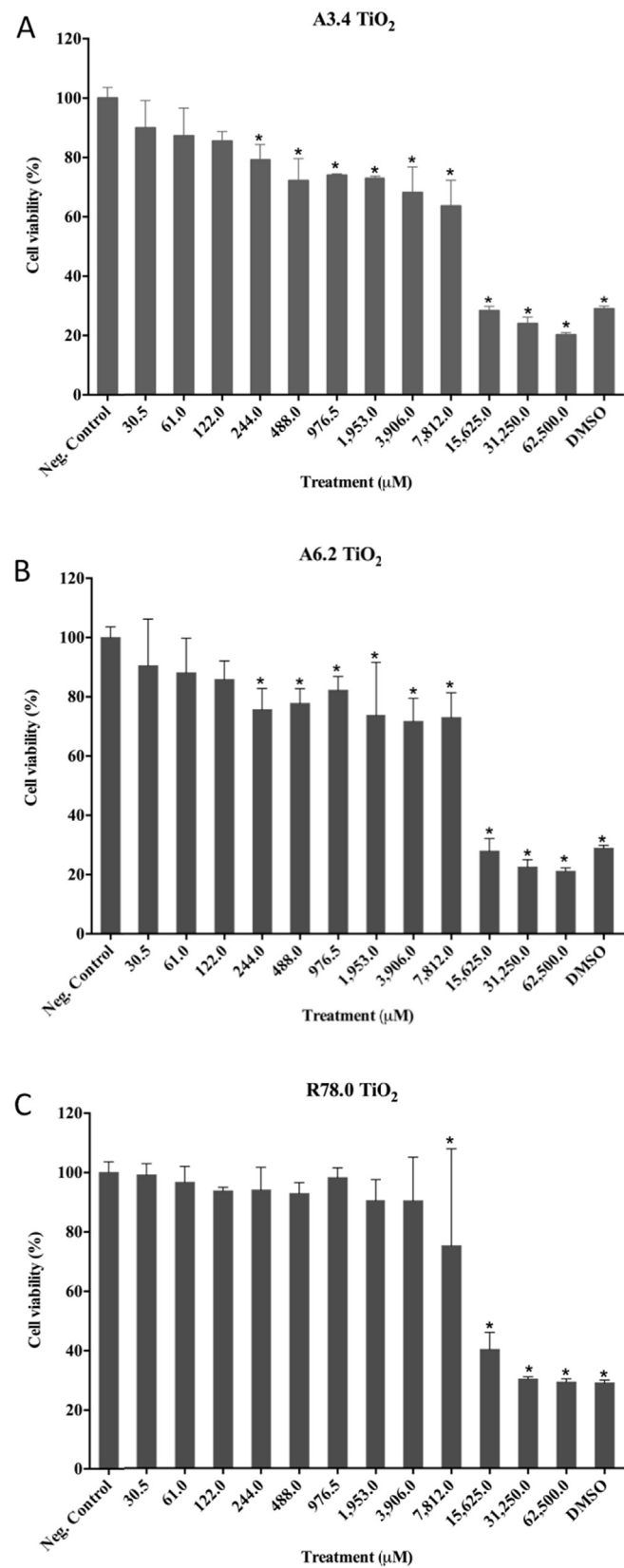


Fig. 3. Effects of TiO₂ NCs on the viability of V79 cells. (A) A3.4; (B) A6.2; (C) R78.0 TiO₂ NCs at concentrations from 30.5 to 62,500.0 μM, negative and positive (DMSO 25%) controls. * Significantly different from negative control ($p < 0.05$).

Table 1
Frequency of micronuclei (MN) and nuclear division index (NDI) observed in V79 cells treated with different concentrations of TiO₂ NCs (A3.4, A6.2 or R78.0) and respective controls.

Treatments (μM)	Frequency of MNs ^a	NDI ^b
	Mean ± SD	Mean ± SD
Negative control	7.00 ± 1.00	1.78 ± 0.03
MMS	45.00 ± 3.61 ^c	1.72 ± 0.04
A3.4 TiO ₂		
30	6.67 ± 1.15	1.78 ± 0.03
60	12.00 ± 1.00	1.77 ± 0.02
120	14.67 ± 2.08 ^c	1.81 ± 0.02
A6.2 TiO ₂		
30	11.33 ± 2.31	1.76 ± 0.03
60	8.33 ± 1.15	1.80 ± 0.05
120	10.00 ± 2.00	1.78 ± 0.01
R78.0 TiO ₂		
976.5	5.33 ± 1.53	1.79 ± 0.01
1956.0	7.67 ± 1.15	1.80 ± 0.05
3906.0	12.33 ± 2.52	1.79 ± 0.03

MMS – Methyl methanesulfonate (400 μM).
^a 3000 binucleated cells were analyzed per treatment group.
^b 1500 cells were analyzed per treatment group.
^c Significantly different from control group ($p < 0.05$).

in vivo have demonstrated that respiratory tract is considered the most affected organ, and that the lung overload is thought to be responsible for the induction of inflammation, ROS production and,

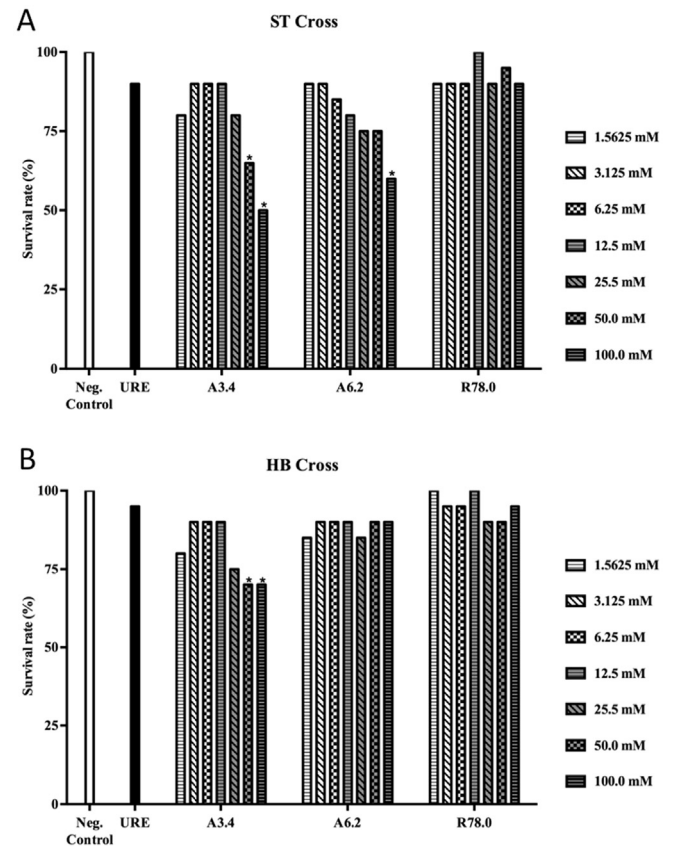


Fig. 4. Survival rates upon exposure to different concentrations of TiO₂ NCs. (A) A3.4; (B) A6.2; (C) R78.0 TiO₂ NCs relative to negative control in the wing Somatic Mutation and Recombination Test in *D. melanogaster*. * Significantly different from negative control ($p < 0.05$).

Table 2

Summary of results obtained with the *Drosophila* wing spot test (SMART) in the marker-heterozygous (MH) progeny of the standard (ST) and high bioactivation (HB) crosses after chronic treatment of larvae with A3.4 TiO₂ NCs.

Genotype, cross and treatment (mM)	Number of flies	Spots per fly (number of spots) statistical diagnosis ^a				Spots with <i>mwh</i> clone ^c	Frequency of clone formation/ 10 ⁵ cells per cell division ^d	
		Small single spots (1–2 cells) ^b	Large single spots (>2 cells) ^b	Twin spots	Total spots		Observed	Control corrected
ST cross								
Negative control	40	0.50 (20)	0.00 (00)	0.00 (00)	0.50 (20)	20	1.02	
URE	40	2.05 (82) +	0.30 (12) +	0.25 (10) +	2.60 (104) +	102	5.23	4.20
A3.4 TiO ₂								
1.5625	40	0.38 (15)–	0.08 (03) i	0.03 (01) i	0.48 (19)–	19	0.97	–0.05
3.125	40	0.38 (15)–	0.15 (06) +	0.05 (02) i	0.58 (23)–	23	1.18	0.15
6.25	40	0.33 (13)–	0.05 (02) i	0.05 (02) i	0.43 (17)–	17	0.87	–0.15
12.5	40	0.53 (21)–	0.08 (03) i	0.00 (00) i	0.60 (24) i	23	1.18	0.15
HB cross								
Negative control	40	0.45 (18)	0.08 (03)	0.05 (02)	0.58 (23)	23	1.18	
URE	40	15.50 (620) +	2.20 (88) +	0.80 (32) +	18.50 (740) +	720	36.89	35.71
A3.4 TiO ₂								
1.5625	40	0.88 (35) +	0.03 (01) i	0.05 (02) i	0.95 (38) +	37	1.90	0.72
3.125	40	1.05 (42) +	0.10 (04) i	0.05 (02) i	1.20 (48) +	47	2.41	1.23
6.25	40	0.55 (22) i	0.15 (06) i	0.08 (03) i	0.78 (31) i	29	1.49	0.31
12.5	40	0.65 (26) i	0.00 (00)–	0.00 (00) i	0.65 (26)–	25	1.28	0.10

Marker *trans*-heterozygous flies (*mwh/fir*³) were evaluated.

^a Statistical diagnoses according to Frei and Würzler (1988, 1995). U test, two sided; probability levels: –, negative; +, positive; i, inconclusive; $p \leq 0.05$ vs. untreated control.

^b Including rare *fir*³ single spots.

^c Considering *mwh* clones from *mwh* single and twin spots.

^d Frequency of clone formation: clones/fly/48,800 cells (without size correction).

ultimately, lung damage (Iavicoli et al., 2012). Therefore, the use of lung cells for assess the TiO₂ NCs genotoxicity *in vitro* is perfectly suitable. On the other hand, by the *in vivo* SMART assay on *D. melanogaster*, we can evaluate the expression of DNA mutations caused by NCs that were ingested by the flies. So, the experimental models of this study were chosen based on different exposure routes and the test organisms available in our laboratory.

Aiming to contribute to the knowledge regarding the potential genotoxicity of TiO₂ NCs, the present study evaluated *in vitro* and *in vivo* three physically well-characterized NCs: anatase TiO₂ of 3.4 and 6.2 nm (A3.4 TiO₂ and A6.2 TiO₂) and a mixed phase nanocrystal 64% rutile/35% brookite/1% anatase TiO₂ of 78.0 nm (R78.0

TiO₂), characterized by high-resolution transmission electron microscopy, X-ray diffraction and Raman spectroscopy. The importance of characterizing testing material has been highlighted by several authors as an elemental part of toxicity studies (Arora et al., 2012; Chen et al., 2014; Nystrom and Fadeel, 2012).

The present study evaluated the cytotoxic potential of anatase TiO₂ NCs through an XTT colorimetric assay with V79 cells. The results showed that both sizes of anatase TiO₂ NCs (3.4 and 6.2 nm) were similarly able to decrease cell viability in a dose-dependent manner. The observed results are in agreement with those observed in A549 human lung carcinoma cells (CCL-185) (Jugan et al., 2012), and mouse macrophages (Ana-1) (Zhang et al.,

Table 3

Summary of results obtained with the *Drosophila* wing spot test (SMART) in the marker-heterozygous (MH) progeny of the standard (ST) and high bioactivation (HB) crosses after chronic treatment of larvae with A6.2 TiO₂ NCs.

Genotype, cross and treatment (mM)	Number of flies	Spots per fly (number of spots) statistical diagnosis ^a				Spots with <i>mwh</i> clone ^c	Frequency of clone formation/ 10 ⁵ cells per cell division ^d	
		Small single spots (1–2 cells) ^b	Large single spots (>2 cells) ^b	Twin spots	Total spots		Observed	Control corrected
ST cross								
Neg. control	40	0.50 (20)	0.00 (00)	0.00 (00)	0.50 (20)	20	1.02	
URE	40	2.05 (82) +	0.30 (12) +	0.25 (10) +	2.60 (104) +	102	5.23	4.20
A6.2 TiO ₂								
1.5625	40	0.53 (21)–	0.08 (03) i	0.05 (02) i	0.65 (26) i	25	1.28	0.26
3.125	40	0.33 (13)–	0.05 (02) i	0.00 (00) i	0.38 (15)–	14	0.72	–0.31
6.25	40	0.50 (20)–	0.05 (02) i	0.00 (00) i	0.55 (22)–	21	1.08	0.05
12.5	40	0.45 (18)–	0.03 (01) i	0.03 (01) i	0.50 (20)–	20	1.02	0.00
HB cross								
Neg. control	40	0.45 (18)	0.08 (03)	0.05 (02)	0.58 (23)	23	1.18	
URE	40	15.50 (620) +	2.20 (88) +	0.80 (32) +	18.50 (740) +	720	36.89	35.71
A6.2 TiO ₂								
1.5625	40	0.65 (26) i	0.10 (04) i	0.05 (02) i	0.80 (32) i	31	1.59	0.41
3.125	40	0.50 (20) i	0.00 (00)–	0.03 (01) i	0.53 (21)–	20	1.02	–0.15
6.25	40	0.50 (20) i	0.00 (00)–	0.03 (01) i	0.53 (21)–	20	1.02	–0.15
12.5	40	0.58 (23) i	0.05 (02) i	0.05 (02) i	0.68 (27)–	27	1.38	0.20

Marker *trans*-heterozygous flies (*mwh/fir*³) were evaluated.

^a Statistical diagnoses according to Frei and Würzler (1988, 1995). U test, two sided; probability levels: –, negative; +, positive; i, inconclusive; $p \leq 0.05$ vs. untreated control.

^b Including rare *fir*³ single spots.

^c Considering *mwh* clones from *mwh* single and twin spots.

^d Frequency of clone formation: clones/fly/48,800 cells (without size correction).

Table 4
Summary of results obtained with the *Drosophila* wing spot test (SMART) in the marker-heterozygous (MH) progeny of the standard (ST) and high bioactivation crosses (HB) after chronic treatment of larvae with R78.0 TiO₂ NCs.

Genotype, cross and treatment (mM)	Number of flies	Spots per fly (number of spots) statistical diagnosis ^a				Spots with <i>mwh</i> clone ^c	Frequency of clone formation/ 10 ⁵ cells per cell division ^d	
		Small single spots (1–2 cells) ^b	Large single spots (>2 cells) ^b	Twin spots	Total spots		Observed	Control corrected
ST cross								
Neg. control	40	0.50 (20)	0.00 (00)	0.00 (00)	0.50 (20)	20	1.02	
URE	40	2.05 (82) +	0.30 (12) +	0.25 (10) +	2.60 (104) +	102	5.23	4.20
R78.0 TiO ₂								
1.5625	40	0.38 (15)–	0.10 (04) i	0.00 (00) i	0.48 (19)–	17	0.87	–0.15
3.125	40	0.53 (21)–	0.10 (04) i	0.03 (01) i	0.65 (26) i	26	1.33	0.31
6.25	40	0.43 (17)–	0.00 (00) i	0.03 (01) i	0.45 (18)–	16	0.82	–0.20
12.5	40	0.48 (19)–	0.08 (03) i	0.10 (04) i	0.65 (26) i	26	1.33	0.31
HB cross								
Neg. control	40	0.45 (18)	0.08 (03)	0.05 (02)	0.58 (23)	23	1.18	
URE	40	15.50 (620) +	2.20 (88) +	0.80 (32) +	18.50 (740) +	720	36.89	35.71
R78.0 TiO ₂								
1.5625	40	0.78 (31) +	0.18 (07) i	0.00 (00) i	0.95 (38) +	38	1.95	0.77
3.125	40	0.68 (27) i	0.13 (05) i	0.08 (03) i	0.88 (35) i	30	1.54	0.36
6.25	40	1.23 (49) +	0.05 (02) i	0.00 (00) i	1.28 (51) +	50	2.56	1.38
12.5	40	0.92 (37) +	0.05 (02) i	0.02 (01) i	1.00 (40) +	40	2.05	0.87

Marker *trans*-heterozygous flies (*mwh/fli³*) were evaluated.

^a Statistical diagnoses according to Frei and Würzler (1988, 1995). U test, two sided; probability levels: –, negative; +, positive; i, inconclusive; $p \leq 0.05$ vs. untreated control.

^b Including rare *fli³* single spots.

^c Considering *mwh* clones from *mwh* single and twin spots.

^d Frequency of clone formation: clones/flies/48,800 cells (without size correction).

2013). The cytotoxic activity of metal oxide particles is often associated with an increase in intracellular reactive oxygen species (ROS) (Nel et al., 2006).

Dimethyl sulfoxide (DMSO) is not commonly used as a positive control for cytotoxicity. It is an aprotic solvent usually used to solubilize a wide variety of poorly soluble polar and nonpolar molecules in permeation assays. Despite increasing the solubility, they have some moderate toxic effects. Some assays have shown that DMSO is highly cytotoxic at concentrations of 20 to 50% (Da Violante et al., 2002; Galvão et al., 2014; Jamalzadeh et al., 2016). However, based on previous reports from *in vitro* studies (Ropero et al., 2009; Uddin et al., 2009; Oliveira et al., 2015; Wakabayashi et al., 2015), we used 25% DMSO as positive control for cytotoxicity. The Cytokinesis Block Micronucleus (CBMN) assay with Chinese hamster lung fibroblasts (V79 cells) was performed with the non-cytotoxic TiO₂ NCs concentrations as previously determined by XTT assay. Among the anatase TiO₂ NCs assessed, only A3.4 at the highest concentration was able to induce MN formation. Therefore, for these experimental conditions, we hypothesize that the genotoxic effects of the anatase phase are dependent on crystal size. Studies using anatase TiO₂ NCs of different sizes have reported conflicting outcomes. Differences in genotoxicity without relationship to dose or size of anatase TiO₂ NCs were shown by Tavares et al. (2014). On the other hand, depending on the experimental conditions, TiO₂ NCs genotoxicity can be highly dependent upon size and shape. For example, TiO₂ anatase NCs (10–20 nm) have shown increase of the MN frequency as a result of chromosomal damage, whilst in the same study this genotoxicity was not induced by 200 nm anatase (Gurr et al., 2005). Genotoxic effects of 30–70 nm anatase TiO₂ NCs induced MN formation in HepG2 cells and revealed a significant concentration-dependent increase in oxidative DNA damage, probably caused by the registered intracellular elevation of ROS (Shukla et al., 2013). Nevertheless, although demonstrating high cytotoxic activity, Guichard et al. (2012) found no significant MN formation after exposing Syrian hamster embryo cells to 14 nm anatase TiO₂ NCs treatment.

Arora et al. (2012) have raised the relevance of *in vivo* studies on nanotoxicology based on validated *in vitro* results despite current

concerns about the use of animals in research, making *in vivo* work more difficult. Currently a global effort has been made to reduce the use of animals in toxicological/genetic research, particularly in regard to the development of alternative *in vivo* models (Siddique et al., 2005). One alternative model, highlighted by Parvathi and Rajagopal (2014), is the fruit fly *D. melanogaster*. The ease of screening phenotypes and their susceptibility for genetic manipulation make *Drosophila* an ideal model for mutagenicity and toxicological screening. Demir et al. (2013) suggested that this *in vivo* eukaryotic model offers many advantages compared to *in vitro* studies or *in vivo* studies using mammals.

The somatic mutation and recombination test (SMART) is extremely sensitive and determines chemical mutagenicity by assessing the loss of heterozygosity (LOH) of cellular markers. This LOH produces single spots (small and large) by point mutation, deletion or non-disjunction and twin spots, which are produced exclusively by mitotic recombination (Graf et al., 1984). For this purpose, two crosses are typically used: the standard (ST) cross and a high bioactivation (HB) cross. The latter is characterized by improved sensitivity to promutagens and procarcinogens owing to the high level of constitutively expressed cytochrome P450 (Frölich and Würzler, 1989; Graf et al., 1989; Graf and van Schaik, 1992).

In the SMART assay of this investigation, no mutagenic effects were observed for individuals originating from the ST cross, as previously observed by Carmona et al. (2015) in a study with nano-TiO₂ and its bulk form. The smallest anatase TiO₂ NCs tested (3.4 nm) induced mutagenic effects on the wings of HB crosses, as well MN formations as related. Although all concentrations of A3.4 TiO₂ induced mutagenic spots, only the effects of the two lowest concentrations were statistically significant. The inconclusive or negative results for total spots observed in the two highest concentrations of A3.4 TiO₂ can be justified in two ways. The increase in NCs concentrations can lead to cell death from mutagenic effects without individual death and consequently an absence of mutant spots in the wings analyzed, or, as suggested by Magdolenova et al. (2013), the increase in the NCs concentrations can enhance NCs agglomeration. NCs agglomerates or aggregates can become approximately 40 times larger than the individual NCs

(Strobel et al., 2014). NCs agglomerates/aggregates could influence biological interactions, such as cellular binding/uptake, cytotoxic and genotoxic effects (Butler et al., 2014; Falck et al., 2009; Janer et al., 2014; Lankoff et al., 2012; Petkovic et al., 2011). The highest size of TiO₂ NCs (6.2 nm) of the same anatase crystalline phase was not mutagenic at any concentration tested. Our findings suggest that the mutagenic effects of anatase TiO₂ NCs are size dependent, considering that only the smallest size (3.4 nm) was able to induce mutagenic effects. Previous SMART assays performed with TiO₂ NCs showed no mutagenic effects for anatase TiO₂ NCs in the ST cross, supporting our results (Carmona et al., 2015; Demir et al., 2013). In our study, positive results were observed only in individuals from HB cross, which exhibits a high constitutive level of cytochrome P450 (Graf and van Schaik, 1992).

In addition to the size evaluation, the crystalline phase of TiO₂ NCs can be considered an important parameter in cytotoxic and genotoxic investigations. For this purpose, the NCs sizes among different crystalline structures must be maintained. Here, we evaluated the effects of a mixed phase of 78.0 nm TiO₂ NCs in which the rutile phase is predominant (64%). The R78.0 TiO₂ NCs were able to induce cytotoxic effects in V79 cells, but no genotoxic effects were observed in the CBMN assay. Although the sizes of anatase TiO₂ NCs and rutile TiO₂ NCs employed in this study were different, we observed higher cytotoxic potential for anatase than for rutile NCs. Some studies have shown that rutile is the most stable phase of TiO₂ NCs (Haines and Leger, 1993; Smijs and Pavel, 2011), and only induced cytotoxic effects at high concentrations. Recent reviews have emphasized the higher photoactivity of anatase NCs compared with rutile NCs (Banerjee, 2011; Smijs and Pavel, 2011). Jiang et al. (2008) showed that the ability of different crystal phases of TiO₂ NCs to generate ROS was higher for anatase than for rutile samples. However, in the present study, we have no parameter to affirm if low cytotoxic effect observed for rutile NCs is due to its higher size (78.0 nm) or due to its crystalline structure.

Negative results on genotoxic effects after rutile TiO₂ exposure have been reported. No significant MN formation was detected in Syrian hamster embryo cells exposed to 62 nm size TiO₂ NCs (Guichard et al., 2012). Similarly, Landsiedel et al. (2010) demonstrated no genotoxicity *in vitro* (Ames' Salmonella gene mutation test and V79 micronucleus chromosome mutation test) or *in vivo* (mouse bone marrow MN test and Comet DNA damage assay in lung cells from rats exposed by inhalation) using rutile TiO₂ NCs (10–50 nm). Falck et al. (2009) showed positive cytotoxic effects and DNA damage associated with nanosized rutile TiO₂, but no significant increase in MN induction in cultured human bronchial epithelial BEAS 2B cells.

Here, NCs containing 64% rutile phase TiO₂ (R78.0 TiO₂) were assessed for the first time by an *in vivo* SMART assay. Our results showed significant mutagenic effects at all concentrations tested, except at 3.125 mM. Mutagenic effects assayed by SMART in this present study were only found in the HB cross. The high intrinsic metabolic activity associated with HB individuals (Graf and van Schaik, 1992), coupled with the oxidative stress triggered by TiO₂ NCs (Gurr et al., 2005; Jugan et al., 2012) and with the impaired ability of cells to repair DNA lesions (Jugan et al., 2012), maybe are the determinants for the appearance of mutant spots in *D. melanogaster* wings.

Our results for the XTT colorimetric assay, *in vitro* micronucleus test and *in vivo* SMART assay revealed either the absence or presence of mutagenic effects, dependent on TiO₂ NCs size and independent of TiO₂ crystalline structure. However, to determine which feature causes the majority of cytotoxic and genotoxic induction, others relevant parameters have to be analyzed, including agglomerate/aggregate formation, hydrodynamic size, zeta potential, and different times of NCs exposure for cultured cells. Without

that, these conflicts in outcomes will continue due to the heterogeneity of samples types being tested and the biological models that are being challenged.

The differences observed in cytotoxic and genotoxicity for closely related NCs highlights the importance of investigating the toxic potential of each one individually, instead of assuming a common mechanism and equal genotoxic effects for a set of similar NCs (Tavares et al., 2014). Furthermore, the major relevance of this diversity of data is the possibility to generate information aimed at corroborating the literature. Nanotechnology is an emerging field and requires further knowledge about safety to people and the environment. According to Arora et al. (2012), experimental results on predictive toxicology can also corroborate with nanomaterials synthesis to help remove toxicity by design parameters.

5. Conclusions

In conclusion, our study demonstrated that anatase TiO₂ NCs of the smallest size were able to induce mutagenic effects *in vitro* and *in vivo*. The larger anatase NCs did not cause DNA damage, despite being only 2.8 nm larger. For rutile TiO₂ NCs, no clastogenic/aneugenic effects were observed in the MN assay. However, the increase in mutagenic spots was significant. In these experimental conditions, we can affirm that both anatase and rutile TiO₂ NCs induce mutagenicity. Therefore, the use of these nanomaterials should be closely monitored and their genotoxicity action mechanisms elucidated.

Conflict of interest statement

The authors declare that there are no conflicts of interest.

Author contributions

A.C.A. Silva and N.O. Dantas were responsible for the synthesis and characterization of TiO₂ NCs. Data were generated by E.M. Reis, P.F. Oliveria and H.D. Nicolella. A.A.A. Rezende, D.C. Tavares and M.A. Spanó contributed to the conceptualization of the project, analyzed the data and prepared the manuscript draft, including figures and tables. All authors approved the final manuscript.

Acknowledgments

This work was supported by Conselho Nacional de Desenvolvimento Científico e Tecnológico (CNPq), Fundação de Amparo à Pesquisa do Estado de Minas Gerais (FAPEMIG), Fundação de Amparo à Pesquisa do Estado de São Paulo (FAPESP), Universidade de Franca (UNIFRAN) and Universidade Federal de Uberlândia (UFU).

Transparency document

Transparency document related to this article can be found online at <http://dx.doi.org/10.1016/j.fct.2016.08.023>.

References

- Abbas, Z., Holmberg, J.P., Hellstrom, A.K., Hagstrom, M., Bergenholtz, J., Hasselov, M., Ahlberg, E., 2011. Synthesis, characterization and particle size distribution of TiO₂ colloidal nanoparticles. *Colloids Surf. A* 384, 254–261.
- Arora, S., Rajwade, J.M., Paknikar, K.M., 2012. Nanotoxicology and *in vitro* studies: the need of the hour. *Toxicol. Appl. Pharmacol.* 258, 151–165.
- Banerjee, A.N., 2011. The design, fabrication, and photocatalytic utility of nanostructured semiconductors: focus on TiO₂-based nanostructures. *Nanotechnol. Sci. Appl.* 4, 35–65.
- Banfield, J.F., Veblen, D.R., 1992. Conversion of perovskite to anatase and TiO₂ (B): a TEM study and the use of fundamental building blocks for understanding

- relationships among the TiO₂ minerals. *Am. Mineral.* 77, 545–557.
- Butler, K.S., Casey, B.J., Garbocauskas, G.V., Dair, B.J., Elespuru, R.K., 2014. Assessment of titanium dioxide nanoparticle effects in bacteria: association, uptake, mutagenicity, co-mutagenicity and DNA repair inhibition. *Mutat. Res. Genet. Toxicol. Environ. Mutagen.* 768, 14–22.
- Carmona, E.R., Escobar, B., Vales, G., Marcos, R., 2015. Genotoxic testing of titanium dioxide anatase nanoparticles using the wing-spot test and the comet assay in *Drosophila*. *Mutat. Res.* 778, 12–21.
- Chen, T., Yan, J., Li, Y., 2014. Genotoxicity of titanium dioxide nanoparticles. *J. Food Drug Anal.* 22, 95–104.
- Cowie, H., Magdolenova, Z., Saunders, M., Drlickova, M., Correia Carreira, S., Halamoda Kenzaoui, B., Gombau, L., Guadagnini, R., Lorenzo, Y., Walker, L., Fjellsbo, L.M., Huk, A., Rinna, A., Tran, L., Volkovova, K., Boland, S., Juillerat-Jeanneret, L., Marano, F., Collins, A.R., Dusinska, M., 2015. Suitability of human and mammalian cells of different origin for the assessment of genotoxicity of metal and polymeric engineered nanoparticles. *Nanotoxicology* 9 (Suppl. 1), 57–65.
- Da Violante, G., Zerrouk, N., Richard, I., Provot, G., Chaumeil, J.C., Arnaud, P., 2002. Evaluation of the cytotoxicity effect of dimethyl sulfoxide (DMSO) on Caco2/TC7 colon tumor cell cultures. *Biol. Pharm. Bull.* 25, 1600–1603.
- de Andrade, L.R., Brito, A.S., Melero, A., Zanin, H., Ceragioli, H.J., Baranauskas, V., Cunha, K.S., Irazusta, S.P., 2014. Absence of mutagenic and recombinogenic activity of multi-walled carbon nanotubes in the *Drosophila* wing-spot test and Allium cepa test. *Ecotoxicol. Environ. Saf.* 99, 92–97.
- Deepa Parvathi, V., Rajagopal, K., 2014. Nanotoxicology testing: potential of *Drosophila* in toxicity assessment of nanomaterials. *Int. J. Nanosci. Nanotechnol.* 5, 25–35.
- Demir, E., Turna, F., Vales, G., Kaya, B., Creus, A., Marcos, R., 2013. In vivo genotoxicity assessment of titanium, zirconium and aluminium nanoparticles, and their microparticulated forms, in *Drosophila*. *Chemosphere* 93, 2304–2310.
- Demir, E., Vales, G., Kaya, B., Creus, A., Marcos, R., 2011. Genotoxic analysis of silver nanoparticles in *Drosophila*. *Nanotoxicology* 5, 417–424.
- Di Carlo, G., Calogero, G., Bruciale, M., Caschera, D., de Caro, T., Di Marco, G., Ingo, G.M., 2014. Insights into meso-structured photoanodes based on titanium oxide thin film with high dye adsorption ability. *J. Alloy. Compd.* 609, 116–124.
- Dobrzynska, M.M., Gajowik, A., Radzikowska, J., Lankoff, A., Dusinska, M., Kruzewski, M., 2014. Genotoxicity of silver and titanium dioxide nanoparticles in bone marrow cells of rats in vivo. *Toxicology* 315, 86–91.
- Eastmond, D.A., Tucker, J.D., 1989. Identification of aneuploidy-inducing agents using cytokinesis-blocked human lymphocytes and an antikinetochore antibody. *Environ. Mol. Mutagen.* 13, 34–43.
- Falck, G.C., Lindberg, H.K., Suhonen, S., Vippola, M., Vanhala, E., Catalan, J., Savolainen, K., Norppa, H., 2009. Genotoxic effects of nanosized and fine TiO₂. *Hum. Exp. Toxicol.* 28, 339–352.
- Fenech, M., 2000. The in vitro micronucleus technique. *Mutat. Res.* 455, 81–95.
- Fenech, M., 2007. Cytokinesis-block micronucleus cytome assay. *Nat. Protoc.* 2, 1084–1104.
- Foth, H., Stewart, J.D., Gebel, T., Bolt, H.M., 2012. Safety of nanomaterials. *Arch. Toxicol.* 86, 983–984.
- Frei, H., Würigler, F.E., 1988. Statistical methods to decide whether mutagenicity test data from *Drosophila* assays indicate a positive, negative, or inconclusive result. *Mutat. Res.* 203, 297–308.
- Frei, H., Würigler, F.E., 1995. Optimal experimental design and sample size for the statistical evaluation of data from somatic mutation and recombination tests (SMART) in *Drosophila*. *Mutat. Res.* 334, 247–258.
- Frölich, A., Würigler, F.E., 1989. New tester strains with improved bioactivation capacity for the *Drosophila* wing-spot test. *Mutat. Res.* 216, 179–187.
- Fu, P.P., Xia, Q., Hwang, H.M., Ray, P.C., Yu, H., 2014. Mechanisms of nanotoxicity: generation of reactive oxygen species. *J. Food Drug Anal.* 22, 64–75.
- Galvão, J., Davis, B., Tilley, M., Normando, E., Duchon, M.R., Cordeiro, M.F., 2014. Unexpected low-dose toxicity of the universal solvent DMSO. *FASEB J.* 28, 1317–1330.
- Gaynor, A.G., Gonzalez, R.J., Davis, R.M., Zallen, R., 1997. Characterization of nano-phase titania particles synthesized using in situ steric stabilization. *J. Mater. Res.* 12, 1755–1765.
- Grabowska, E., Diak, M., Marchelek, M., Zaleska, A., 2014. Decahedral TiO₂ with exposed facets: synthesis, properties, photoactivity and applications. *Appl. Catal. B Environ.* 156, 213–235.
- Graf, U., Frei, H., Kagi, A., Katz, A.J., Würigler, F.E., 1989. Thirty compounds tested in the *Drosophila* wing spot test. *Mutat. Res.* 222, 359–373.
- Graf, U., van Schaik, N., 1992. Improved high bioactivation cross for the wing somatic mutation and recombination test in *Drosophila melanogaster*. *Mutat. Res.* 271, 59–67.
- Graf, U., Würigler, F.E., Katz, A.J., Frei, H., Juon, H., Hall, C.B., Kale, P.G., 1984. Somatic mutation and recombination test in *Drosophila melanogaster*. *Environ. Mutagen* 6, 153–188.
- Guichard, Y., Schmit, J., Darne, C., Gate, L., Goutet, M., Rousset, D., Rastoix, O., Wrobel, R., Witschger, O., Martin, A., Fierro, V., Binet, S., 2012. Cytotoxicity and genotoxicity of nanosized and micro-sized titanium dioxide and iron oxide particles in Syrian hamster embryo cells. *Ann. Occup. Hyg.* 56, 631–644.
- Guinier, A., 1963. X-ray Diffraction in Crystals, Imperfect Crystals, and Amorphous Bodies. W.H. Freeman, San Francisco.
- Gurr, J.R., Wang, A.S., Chen, C.H., Jan, K.Y., 2005. Ultrafine titanium dioxide particles in the absence of photoactivation can induce oxidative damage to human bronchial epithelial cells. *Toxicology* 213, 66–73.
- Guzmán-Rincón, J., Graf, U., 1995. *Drosophila melanogaster* somatic mutation and recombination test as a biomonitor. In: Butterworth, F.M., Corkum, L.D., Guzmán-Rincón, J. (Eds.), *Biomonitoring and Biomarkers as Indicators of Environmental Change*. Plenum Press, New York, pp. 169–181.
- Haines, J., Leger, J.M., 1993. X-ray diffraction study of TiO₂ up to 49 GPa. *Phys. B* 192, 233–237.
- IARC, 2010. Carbon Black, Titanium Dioxide, and talc. IARC Monographs on the Evaluation of Carcinogenic Risks to Humans. World Health Organization - International Agency on Cancer Research, Lyon, France.
- Iavicoli, I., Leso, V., Bergamaschi, A., 2012. Toxicological effects of titanium dioxide nanoparticles: a review of in vivo studies. *J. Nanomater.* 36. Article ID 964381.
- Jamalzadeh, L., Ghafouri, H., Sariri, R., Rabuti, H., Nasirzade, J., Hasani, H., Aghamaali, M.R., 2016. Cytotoxic effects of some common organic solvents on MCF-7, RAW-264.7 and human umbilical vein endothelial cells. *Avicenna. J. Med. Biochem.* 4 e33453.
- Janer, G., Mas Del Molino, E., Fernandez-Rosas, E., Fernandez, A., Vazquez-Campos, S., 2014. Cell uptake and oral absorption of titanium dioxide nanoparticles. *Toxicol. Lett.* 228, 103–110.
- Jiang, J., Oberdorster, G., Elder, A., Gelein, R., Mercer, P., Biswas, P., 2008. Does nanoparticle activity depend upon size and crystal phase? *Nanotoxicology* 2, 33–42.
- Jugan, M.L., Barillet, S., Simon-Deckers, A., Herlin-Boime, N., Sauvaigo, S., Douki, T., Carriere, M., 2012. Titanium dioxide nanoparticles exhibit genotoxicity and impair DNA repair activity in A549 cells. *Nanotoxicology* 6, 501–513.
- Juillerat, L., Fjellsbo, L.M., Dusinska, M., Collins, A.R., Handy, R., Riediker, M., 2015. Biological impact assessment of nanomaterial used in nanomedicine. Introduction to the NanoTEST project. *Nanotoxicology* 9, 5–12.
- Kastenbaum, M.A., Bowman, K.O., 1970. Tables for determining the statistical significance of mutation frequencies. *Mutat. Res.* 9, 527–549.
- Koo, B., Park, J., Kim, Y., Choi, S.H., Sung, Y.E., Hyeon, T., 2006. Simultaneous phase- and size-controlled synthesis of TiO₂ nanorods via non-hydrolytic sol-gel reaction of syringe pump delivered precursors. *J. Phys. Chem. B* 110, 24318–24323.
- Landsiedel, R., Kapp, M.D., Schulz, M., Wiench, K., Oesch, F., 2009. Genotoxicity investigations on nanomaterials: methods, preparation and characterization of test material, potential artifacts and limitations—many questions, some answers. *Mutat. Res.* 681, 241–258.
- Landsiedel, R., Ma-Hock, L., Van Ravenzwaay, B., Schulz, M., Wiench, K., Champ, S., Schulte, S., Wohlleben, W., Oesch, F., 2010. Gene toxicity studies on titanium dioxide and zinc oxide nanomaterials used for UV-protection in cosmetic formulations. *Nanotoxicology* 4, 364–381.
- Lankoff, A., Sandberg, W.J., Wegierek-Ciuk, A., Lisowska, H., Refsnes, M., Sartowska, B., Schwarze, P.E., Meczynska-Wielgosz, S., Wojewodzka, M., Kruzewski, M., 2012. The effect of agglomeration state of silver and titanium dioxide nanoparticles on cellular response of HepG2, A549 and THP-1 cells. *Toxicol. Lett.* 208, 197–213.
- Li, Y., Zhang, Y., Yan, B., 2014. Nanotoxicity overview: nano-threat to susceptible populations. *Int. J. Mol. Sci.* 15, 3671–3697.
- Lindberg, H.K., Falck, G.C., Catalan, J., Koivisto, A.J., Suhonen, S., Jarventaus, H., Rossi, E.M., Nykasenoja, H., Peltonen, Y., Moreno, C., Alenius, H., Tuomi, T., Savolainen, K.M., Norppa, H., 2012. Genotoxicity of inhaled nanosized TiO₂ in mice. *Mutat. Res.* 745, 58–64.
- Lombardot, B., Oh, C.T., Kwak, J., Genovesio, A., Kang, M., Hansen, M.A.E., Han, S.J., 2015. High-throughput in vivo genotoxicity testing: an automated readout system for the somatic mutation and recombination test (SMART). *PLoS One* 10 (4), e0121287.
- Magdolenova, Z., Collins, A., Kumar, A., Dhawan, A., Stone, V., Dusinska, M., 2013. Mechanisms of genotoxicity. A review of in vitro and in vivo studies with engineered nanomaterials. *Nanotoxicology* 1–46.
- Nel, A., Xia, T., Madler, L., Li, N., 2006. Toxic potential of materials at the nanolevel. *Science* 311, 622–627.
- Newman, M.D., Stotland, M., Ellis, J.I., 2009. The safety of nanosized particles in titanium dioxide- and zinc oxide-based sunscreens. *J. Am. Acad. Dermatol.* 61, 685–692.
- Nystrom, A.M., Fadeel, B., 2012. Safety assessment of nanomaterials: implications for nanomedicine. *J. Control. Release* 161, 403–408.
- Ohsaka, T., 1980. Temperature-dependence of the Raman-spectrum in anatase TiO₂. *J. Phys. Soc. Jpn.* 48, 1661–1668.
- Oliveira, P.F., Alves, J.M., Damasceno, J.L., Oliveira, R.A.M., Dias, H.J., Crotti, A.E.M., Tavares, D.C., 2015. Cytotoxicity screening of essential oils in cancer cell lines. *Rev. Bras. Farmacogn.* 25, 183–188.
- Pandey, U.B., Nichols, C.D., 2011. Human disease models in *Drosophila melanogaster* and the role of the fly in therapeutic drug discovery. *Pharmacol. Rev.* 63, 411–436.
- Parvathi, V.D., Rajagopal, K., 2014. Nanotoxicology testing: potential of *Drosophila* in toxicity assessment of nanomaterials. *Int. J. Biomed. Nanosci. Nanotechnol.* 5, 25–35.
- Petkovic, J., Zegura, B., Stevanovic, M., Drnovsek, N., Uskokovic, D., Novak, S., Filipic, M., 2011. DNA damage and alterations in expression of DNA damage responsive genes induced by TiO₂ nanoparticles in human hepatoma HepG2 cells. *Nanotoxicology* 5, 341–353.
- Pottier, A., Chaneac, C., Tronc, E., Mazerolles, L., Jolivet, J.-P., 2001. Synthesis of brookite TiO nanoparticles by thermolysis of TiCl₃ in strongly acidic aqueous media. *J. Mat. Chem.* 11, 1116–1121.
- Reis, É.D.M., Rezende, A.A.A.d., Santos, D.V., Oliveria, P.F.d., Nicolella, H.D.,

- Tavares, D.C., Silva, A.C.A., Dantas, N.O., Spanó, M.A., 2015. Assessment of the genotoxic potential of two zinc oxide sources (amorphous and nanoparticles) using the in vitro micronucleus test and the in vivo wing somatic mutation and recombination test. *Food Chem. Toxicol.* 84, 55–63.
- Ropero, A.B., Juan-Picó, P., Rafacho, A., Fuentes, E., Bermúdez-Silva, F.J., Roche, E., Quesada, I., Fonseca, F.R., Nadal, A., 2009. Rapid non-genomic regulation of Ca^{2+} signals and insulin secretion by PPAR α ligands in mouse pancreatic islets of Langerhans. *J. Endocrinol.* 200, 127–138.
- Shakeel, M., Jabeen, F., Shabbir, S., Asghar, M.S., Khan, M.S., Chaudhry, A.S., 2016. Toxicity of nano-titanium dioxide (TiO₂-NP) through various routes of exposure: a review. *Biol. Trace Elem. Res.* 172, 1–36.
- Shukla, R.K., Kumar, A., Gurbani, D., Pandey, A.K., Singh, S., Dhawan, A., 2013. TiO₂ nanoparticles induce oxidative DNA damage and apoptosis in human liver cells. *Nanotoxicology* 7, 48–60.
- Siddique, H.R., Chowdhuri, D.K., Saxena, D.K., Dhawan, A., 2005. Validation of *Drosophila melanogaster* as an in vivo model for genotoxicity assessment using modified alkaline Comet assay. *Mutagenesis* 20, 285–290.
- Smijs, T.G., Pavel, S., 2011. Titanium dioxide and zinc oxide nanoparticles in sunscreens: focus on their safety and effectiveness. *Nanotechnol. Sci. Appl.* 4, 95–112.
- Strobel, C., Torrano, A.A., Herrmann, R., Malissek, M., Brauchle, C., Reller, A., Treuel, L., Hilger, I., 2014. Effects of the physicochemical properties of titanium dioxide nanoparticles, commonly used as sun protection agents, on microvascular endothelial cells. *J. Nanopart. Res.* 16, 2130.
- Tavares, A.M., Louro, H., Antunes, S., Quarre, S., Simar, S., De Temmerman, P.J., Verleysen, E., Mast, J., Jensen, K.A., Norppa, H., Nesselny, F., Silva, M.J., 2014. Genotoxicity evaluation of nanosized titanium dioxide, synthetic amorphous silica and multi-walled carbon nanotubes in human lymphocytes. *Toxicol. in Vitro* 28, 60–69.
- Uddin, S.J., Grice, I.D., Tiralongo, E., 2011. Cytotoxic effects of Bangladeshi medicinal plant extracts. *Evid. Based Complement Alternat. Med.* 2011, ID 578092.
- Vales, G., Demir, E., Kaya, B., Creus, A., Marcos, R., 2013. Genotoxicity of cobalt nanoparticles and ions in *Drosophila*. *Nanotoxicology* 7, 462–468.
- Wakabayashi, K.A.L., Melo, N.I., Aguiar, D.P., Oliveira, P.F., Groppo, M., Silva Filho, A.A., Rodrigues, V., Cunha, W.R., Tavares, D.C., Magalhães, L.G., Crotti, A.E.M., 2015. Anthelmintic effects of the essential oil of fennel (*Foeniculum vulgare* Mill., Apiaceae) against *Schistosoma mansoni*. *Chem. Biodivers.* 12, 1105–1114.
- Weir, A., Westerhoff, P., Fabricius, L., Hristovski, K., von Goetz, N., 2012. Titanium dioxide nanoparticles in food and personal care products. *Environ. Sci. Technol.* 46, 2242–2250.
- Wu, M., Lin, G., Chen, D., Wang, G., He, D., Feng, S., Xu, R., 2002. Sol-hydrothermal synthesis and hydrothermally structural evolution of nanocrystal titanium dioxide. *Chem. Mater* 14, 1974–1980.
- Yu, J., Yu, J.C., Leung, M.K.P., Ho, W., Cheng, B., Zhao, X., Zhao, J., 2003. Effects of acidic and basic hydrolysis catalysts on the photocatalytic activity and microstructures of bimodal mesoporous titania. *J. Catal.* 217, 69–78.
- Yu, J.X., Li, T.H., 2011. Distinct biological effects of different nanoparticles commonly used in cosmetics and medicine coatings. *Cell Biosci.* 1, 19.
- Zhang, J., Song, W., Guo, J., Zhang, J., Sun, Z., Li, L., Ding, F., Gao, M., 2013. Cytotoxicity of different sized TiO₂ nanoparticles in mouse macrophages. *Toxicol. Ind. Health* 29, 523–533.
- Zhang, W.F., He, Y.L., Zhang, M.S., Yin, Z., Chen, Q., 2000. Raman scattering study on anatase TiO₂ nanocrystals. *J. Phys. D. Appl. Phys.* 33, 912–916.